Indirect interactions of metal nanoparticles through graphene

Li-Wei Huang [a], Horng-Tay Jeng [b, c, a, *], Wei-Bin Su [a], Chia-Seng Chang [a, **]

[a] Institute of Physics, Academia Sinica, Taipei, 11529, Taiwan
[b] Department of Physics, National Tsing Hua University, Hsinchu, 30013, Taiwan
[c] Physics Division, National Center for Theoretical Sciences, Hsinchu, 30013, Taiwan

ARTICLE INFO

ABSTRACT

We employ ultra-high vacuum electron microscopy to investigate the interaction of metal nanoparticles through graphene. The nanoparticles attract those on the other side of graphene in the systems of Ag/graphene/Ag and Cu/graphene/Cu. In contrast, the system of Au/graphene/Au manifests the repelling interaction. Our density functional theory calculations demonstrate that for lower electron-affinity metals such as Cu and Ag, the clusters on opposite sides of graphene prefer the same site to share the electron-loss and reduce the energy. While for higher electron-affinity metals such as Au, they prefer to stay away from the clusters on the other side of graphene.
© 2020 The Author(s). Published by Elsevier Ltd. This is an open access article under the CC BY-NC-ND license (http://creativecommons.org/licenses/by-nc-nd/4.0/).

1. Introduction

Unique properties of graphene on electronic, optical and thermal aspects, have been largely explored in the scientific community focusing on their electronic structure and mechanical responses [1,2]. When combining with metal nanoparticles, the hybrid system has generated considerable interests on catalysis [3,4], biomedicine [5,6], optics [7,8] and energy [9,10] applications. Recently, we demonstrated that a significant amount of charge transferred from a single Cu nanoparticle to graphene membrane and caused the redistribution of local electrons [11]. In light of utilizing both sides of a graphene that can usher in novel applications, we were motivated to interrogate whether the adsorption on one side of graphene would affect formation of nanoparticles on the opposite side. Scientists nowadays look for a mechanism to align circuits, such as carbon nanotubes, through graphene membrane to target more advanced nanoscale devices. The attracting mechanism should promise to align nano-electrodes through a membrane to further assemble 1D and 2D nano-objects into the well-defined 3D functional [13–16]. Moreover, conventional nanoparticles are monometallic or bimetallic, such as alloy, core-shell, fused-cluster.

These conventional forms of nanoparticle have also contributed for a variety of applications and impacted our daily life [3–10]. The resultant metal/graphene/metal (M/G/M) nanostructures should be considered as novel forms of nanoparticle or nanocomposites as distinct from conventional configurations [17,18], which will gather prospects and benefits owing to the new possibilities, enhancement and applications.

In this study, we employ the ultra high vacuum transmission electron microscopy (UHV-TEM) to record the formation behavior of metal nanoparticles on both sides of graphene. Our results reveal that M/G/M system indeed existed indirect particle interaction through the graphene, and the interaction is attractive for Ag and Cu nanoparticles but repulsive for Au nanoparticles. We have also performed ab-initio calculations based on density functional theory (DFT) to disclose the origin of these contrasting behaviors for different metal particles. We found for Cu and Ag with lower electron affinity than that of carbon, the charges transferred from metal particles to graphene. It is, therefore, energetically favorable with metal particles on the two sides to share the electron loss by stacking themselves at the same site. On the contrary, Au with a higher electron affinity than graphene extracts electrons from graphene. Hence the Au particles on opposite sides of graphene tend to stay apart in order to acquire more electrons from another region of graphene. We further investigate the correlations among the metal particle, site-preference, Dirac point energy, charge transfer direction, and relative total energy for M/G/M systems to resolve the opposite behaviors of the Cu, Ag, and Au particles.

* Corresponding author. Institute of Physics, Academia Sinica, Taipei, 11529, Taiwan.
** Corresponding author.
E-mail addresses: jeng@phys.nthu.edu.tw (H.-T. Jeng), jasonc@phys.sinica.edu.tw (C.-S. Chang).

Similar charge transfer trend can also be found in metal thin film/graphene systems [12].

2. Materials and methods

Graphene used in the study was produced on a 25 μm thick Cu foil (Alfa Aesar, 99.8% purity) by the chemical vapor deposition [19]. The suspended graphene sheets were transferred on TEM copper grids [20]. The experiments were carried out in a UHV-TEM (JEOL JEM-2000V, the base pressure of specimen chamber is below 5×10^{-8} Pa), which avoided oxidation during the annealing. Since it is known the contaminations will affect the growth of metal nanoparticles, the graphene substrate before metal deposition was cleaned with a conductive heater (JEOL EM-21240, RT to 900 °C) on the sample holder under low level of H_2 environment at 700 °C to remove all the contaminants. More detailed cleaning procedure can be found in Ref. [21]. A homemade nano-positioning system with gold tip electrode is connected to a computer-controlled Keithley 2400 source meter (Fig. S1) [22]. In-situ deposition of high purity metals (Ag, Cu and Au, 99.99%, Nilaco) onto a suspended graphene was carried out with a highly collimated e-beam evaporator (Omicron, UHV EFM3/4). All TEM images were acquired under an accelerating voltage of 80 kV with an electron dose rate less than 1217 electrons/$nm^2 \cdot s$ to prevent the radiation damage. Metal depositions with illumination of e-beam or without have been examined and no apparent differences have been found.

The electronic structure calculations were performed using the full-potential projected augmented wave method [23,24] as implemented in the Vienna ab-initio simulation package (VASP) [25,26] with the exchange−correlation functional described in the Perdew−Burke−Ernzerhof (PBE) form [27]. To simulate the metal (M = Cu, Ag, Au) cluster/graphene/M cluster system, we adopted a 6x6 supercell of graphene with a vacuum thickness over 15 Å. The two pyramidal M clusters on both side of graphene move from the same site toward different sites as shown respectively in Fig. 5(a) and (b) with an indicating offset parameter from 0 to 1. The M cluster contains 11 atoms with seven in the basal plane of the pyramid contacting the graphene, three atoms in the middle plane, and one M atom at the tip of the pyramid. The M atoms in the basal plane situate at the hollow site of the graphene honeycomb structure. The geometry of the considered Cu, Ag, Au systems with 94 atoms therein is optimized separately for each offset parameter with the total energies converged within 0.001 eV/cell. The geometry optimizations were performed separately with and without Van der Waals correction. Both results are very close to each other, which indicates that the main driving force in our system is the strong charge transfer effect (see discussions below) rather than the weak Van der Waals force. The former is about one order of magnitude stronger than the latter in our calculations. The self-consistent calculations and the geometry optimization are performed on a $6 \times 6 \times 1$ Monkhorst-Pack k-point mesh (20 k-points) with the cutoff energy of 400 eV.

To explore the driving force of the attraction and repulsion between metal clusters observed in our experiments, we adopted 2 model systems with 2 metal clusters located at the same and different positions on both side of graphene as depicted in Fig. 5(a) and (b), respectively. For the former case that the centers of 2 metal clusters stay at the same horizontal position (Fig. 5(a)), we set the offset parameter = 0. As for the latter case that 2 metal clusters locate at different horizontal places (Fig. 5(b)), the offset parameter = 1. We than move the upper metal cluster from the position in Fig. 5(a) to that in Fig. 5(b) in 10 steps with the lower metal cluster fixed at the original place, and calculate the relative total energy in each step as shown in Fig. 5(c). Take the intermediate distance with offset parameter = 0.5 for example, the horizontal distance

between the centers of 2 metal clusters is equal to 1/2 of that in the offset parameter = 1 case (Fig. 5(b)).

3. Results and discussion

We deposited two monolayers (ML) of Ag onto the membrane and heated at 500 °C in the UHV chamber. Nanoparticles with a size of about 10 nm in diameter (dia.) were formed on one side of the membrane. The membrane holder was subsequently flipped over in vacuum and then 0.8 ML Ag was deposited on the other side of membrane at room temperature (RT), which form particles with a smaller size of about 3 nm dia. The TEM image Fig. 1(a) clearly demonstrates that after two-side depositions at different temperatures, the bigger Ag nanoparticles (some marked by up arrows) adsorbed on one side (named side A) with a lower density and smaller Ag ones (some marked by horizontal arrows) adsorbed on the other side (named side B) with a higher density. The sample was post-heated again up to 600 °C, and Fig. 1(b) displays steady big nanoparticles remain on side A and small nanoparticles on side B were transformed into big nanoparticles.

Moreover, nanoparticles on side B were located where the big nanoparticles were on the side A. The observation reveals that big nanoparticles on side A apparently attracted the nanoparticles on side B. Three images at right-hand side of Fig. 1(b) are zoom-in images of three representative regions indicated by dashed squares in Fig. 1(b). They display that in the middle of the particles on side A, there appear additionally obvious contours and deeper contrasted shadows that are the reflections of particles on side B. Therefore, the attracting interaction is manifested in the Ag/Graphene/Ag adsorption process.

We further explore this phenomenon for the Cu/graphene/Cu system. We deposited 2 ML coverage of Cu onto the membrane and followed by heating with 0.1 mW DC power, using the probe heating (Fig. S1) [22], to fabricate bigger Cu nanoparticles about 12 nm dia. on side A. The alternative heating method employed here was to detect any driving force due to the heating current. After flipping the membrane in vacuum smaller Cu nanoparticles of about 3 nm were created on side B by depositing 0.8 ML Cu at room temperature (RT). Fig. 2(a) displays the results that bigger Cu nanoparticles adhered on side A and small ones on side B. The sample was heated again to drive the M/G/M interactions by increasing the electric power. After the sample was heated with 0.085 and 0.18 mW, the number of small nanoparticles on side B reduced with the power and gathered at the locations where Cu nanoparticles had already stood on side A. Although the sample temperature with the power provided was not known exactly, the moving speed of the particles recorded under the microscope indicated the sample temperature was close to 600 C at 0.18 mW. The details of the aligning interaction were highlighted by zoom-in imaging below Fig. 2(a−c). From the sequential recorded images, the direction of electric current cause no effect, so the driving force here was purely thermal.

In contrast to the Ag/graphene/Ag and Cu/Graphene/Cu systems, the Au/graphene/Au exhibited entirely different interacting behavior. We followed the same procedure to prepare bigger Au nanoparticles with low density on side A and small ones with high density on side B. After annealing to 600 °C, although small nanoparticles on side B aggregated into larger particles, the distribution of these nanoparticles was random and they were not attracted by the nanoparticles on side A as pervious two cases. Therefore, Au nanoparticles separated by graphene might have no interaction or even repulsive interaction. In order to investigate whether the repulsive interaction does exit, we deposited a higher coverage (4 ML) of Au at RT on both sides of graphene. Under this situation, the TEM image can clearly reveal the overlaps of nanoparticles on
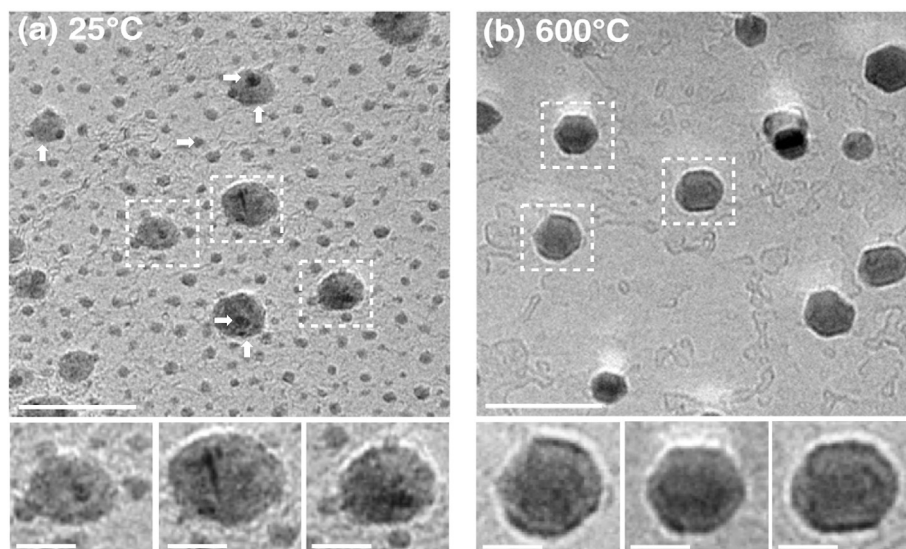
Fig. 1. Ag/Graphene/Ag (a) Large and small Ag nanoparticles on either side of graphene membrane at room temperature. Large particles marked by up arrows on side A and smaller particles marked by horizontal arrows on side B. **(b)** Ag nanoparticles can self-align after they are heated to 600 °C, three zoom-in TEM images highlight Ag nanoparticles on A and B sides align up on the membrane, scale bar = 20 nm. The zoom-in images on below providing higher image contrast; scale bar = 5 nm.
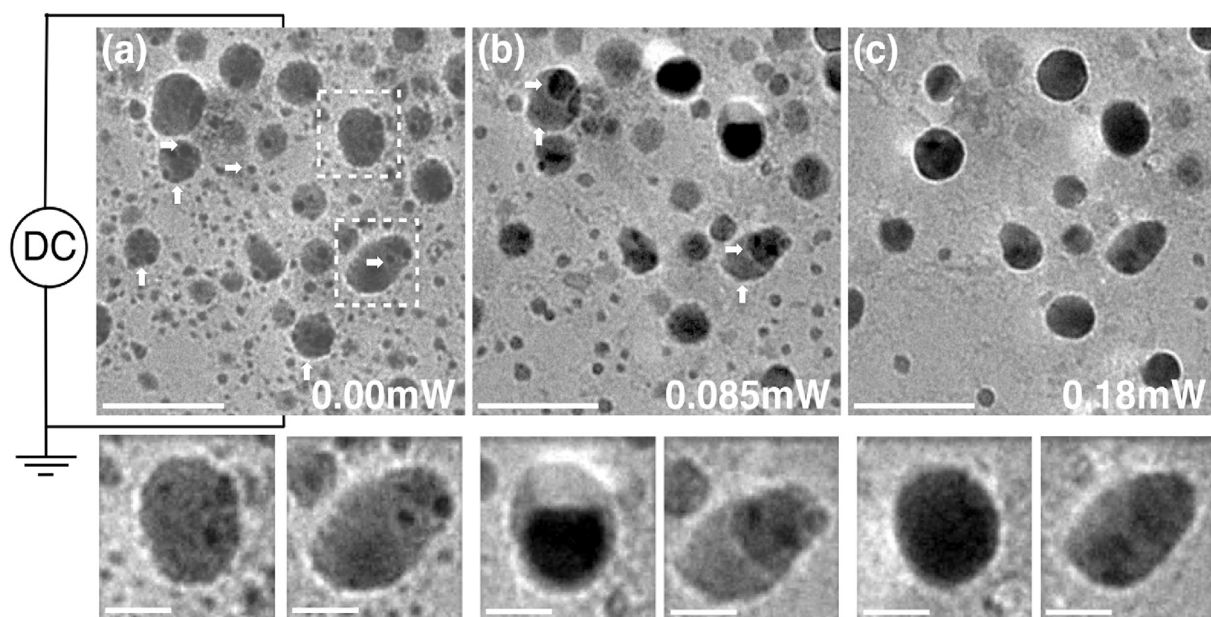

Fig. 2. Cu/Graphene/Cu (a) Large and small Cu nanoparticles deposited on both side of graphene membrane; scale bar = 20 nm. **(b)** The aligning behavior of Cu/Graphene/Cu was driven by electric power of 0.085 mW; scale bar = 20 nm. Large particles marked by up arrows on side A and smaller particles marked by horizontal arrows on side B. **(c)** The aligning behavior of Cu/Graphene/Cu with electric power of 0.18 mW; scale bar = 20 nm. The zoom-in images below providing higher image contrast; scale bar = 5 nm.

two sides, shown in Fig. 3(a). The sample is then subject to heating at 600 °C and we observe the nanoparticle's density is reduced and the inceptive overlaps disappear as in Fig. 3(b). Zoom-in images at the right-hand side of Fig. 3(b) show no overlap in various regions, strongly indicating the existence of repulsive interaction between Au nanoparticles through graphene.

The shadow deposition method (Fig. S2) was further employed to illustrate this repulsive interaction of Au clusters through graphene. Fig. 4(a) shows only one side deposition of Au on the membrane and Fig. 4(b) represents depositions of Au on both sides of the membrane at room temperature. Post-annealing the membrane to 600 °C, Fig. 4(c) dipicts dramatically different morphologies of the Au/

Graphene on the left region and the Au/Graphene/Au on the right. In the Au/Graphene region, the nanoparticles migrated and coalesced. However, in the Au/Graphene/Au region with M/G/M interaction, the nanoparticles repelled each other through the membrane with a much higher density. The phenomenon highlights the strong indirect interaction of Au nanoparticles separated by graphene. Besides the graphene system, our preliminary experiments on another 2D system such as MoS$_2$ also detected the indirect interaction of metal nanoparticles through the monolayer.

Our experimental results reveal two opposite interactive phenomena between noble metal nanoparticles through graphene, which cannot be explained away by the simple electrostatic force. To
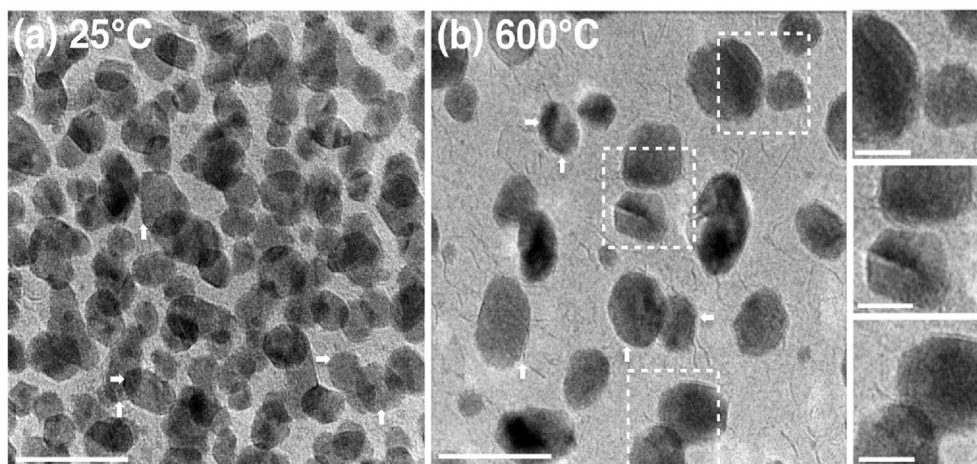
Fig. 3. Au/Graphene/Au (a) A large amount of Au nanoparticles deposited on the either side of the membrane existing obvious overlaps. **(b)** Au/Graphene/Au displayed repelling behaviors and the overlaps no longer existing after the furnace heating, three zoom-in TEM images highlight the repelling behavior across the membrane, scale bar = 20 nm. The zoom-in images of dashed regions in (b) from top to bottom on the right, providing higher image contrast; scale bar = 5 nm.
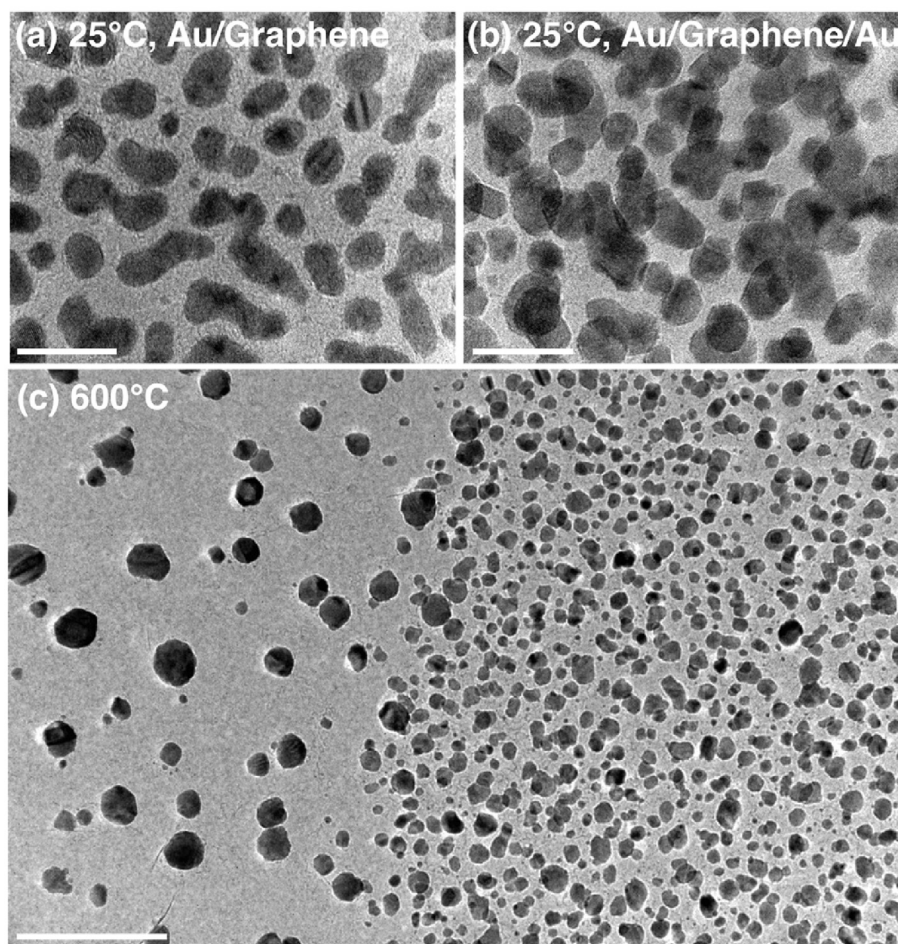

Fig. 4. Au/Graphene and Au/Graphene/Au (a) Au nanoparticles on single side of graphene at RT, scale bar = 20 nm. **(b)** Au nanoparticles on both sides of graphene at RT, scale bar = 20 nm. **(c)** After 600 °C annealing, the same membrane demonstrates two dramatic different morphologies of Au/Graphene without M/G/M interaction on the left hand side and Au/Graphene/Au with M/G/M interaction on the right, scale bar = 200 nm.

resolve the origin of such dramatic behavior, we thus performed first-principles total energy calculations for Cu, Ag, Au clusters on both sides of graphene with the metal clusters moving from the same site (hereafter named on-site) toward different sites (off-site)

as shown in Fig. 5(a) and (b), respectively. We calculated relative total energy with respect to the on-site case, Dirac point (DP) energy, and charge transfer (CT) from metal clusters to graphene for M/graphene/M with metal particles M = Cu, Ag, Au marching from on-
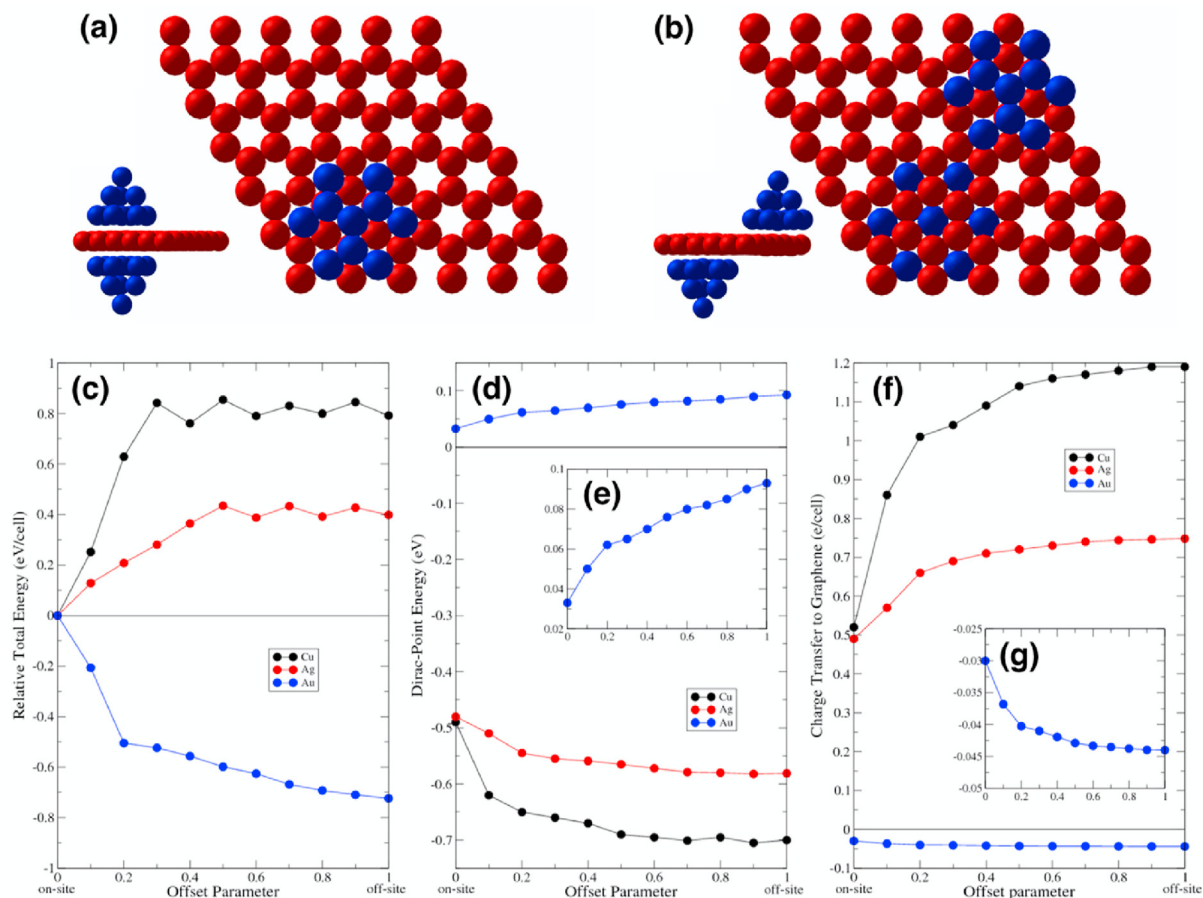
Fig. 5. **Model and calculations for M/graphene/M (a)** The metal clusters (blue) locate at the same site (on-site) of graphene (red). **(b)** The metal clusters locate at different sites (off-site). Calculated relative total energy difference (with respect to the on-site case). **(c)** Dirac point energy **(d,e)** and charge transfer (CT) **(f,g)** for M/graphene/M with metal particles M = Cu, Ag, Au at the same site (on-site) and different sites (off-site). The horizontal axis is the offset parameter from the on-site (offset = 0) to the off-site (offset = 1) case. The CT from metal particles to graphene is defined as positive. (A colour version of this figure can be viewed online.)

site to off-site with the indicating offset parameter running from 0 to 1. In our DFT calculations, due to extremely large computational demand, we have used a supercell of 15 Å × 15 Å × 25 Å, including nearly 100 atoms (22 metal atoms + 72C atoms) and 530 valence electrons. For each data point in Fig. 5(c) (33 data points in total), we have done geometric optimization of the whole system using quantum calculations. For the Cu and Ag cases, as the offset parameter (horizontal axis) goes from 0 to 1, the DFT calculations show a relative higher total energy for the metal clusters locate at different sites (Fig. 5(c)), indicating the attractive nature of the Cu and Ag particles. This agrees well with the experimental observation that the Cu and Ag metal nanoparticles migrate to the same site under annealing to lower the total energy. Around the offset parameter of 0.3 for Cu and 0.5 for Ag, the increasing trend quickly saturates with ~0.8eV and ~0.4eV higher in total energies, respectively. After the saturation, both the total energy curves exhibit slight oscillations with the same periodicity, presumably due to the atomic site effect at the metal particle-graphene interface. On the contrary, our DFT calculations give a lower relative total energy for Au clusters at different sites, indicating the repulsive nature of Au clusters. These DFT conclusions agree excellently with our experimental findings that Cu and Ag nanoparticles attract whereas Au nanoparticles repel each other.

To pursue the driving force of such opposite trends in the cases of Cu(Ag) and Au nanoparticles, we performed electronic structure calculations as shown in the Supplementary Information (SI) S3, S4, and S5 [22]. The band structures and density of states of the on-site

and off-site Cu/graphene/Cu are basically similar to the one of the single side Cu/graphene in our previous work [11]. We further analyzed the Dirac point energy and charge transfer from metal particles to graphene as shown in Fig. 5 (d,e) and (f,g), which were derived from the band structures and density of states in SI S3-5. The Dirac point for Cu clusters at the same site is ~ -0.5eV, which is ~0.2eV higher than ~ -0.7eV for Cu clusters at different site. The lower DP of the off-site case indicates stronger charge transfer of ~1.19e/cell from Cu clusters to graphene (Fig. 5(f)), because of the more contacting graphene atoms that can extract more electrons from the Cu particles. The Cu clusters at the same site thus suffer less electron loss ~0.52e/cell and result in a lower total energy.

The same scenario also applies to the Ag counterparts. As shown in Fig. 5(d), similar charge transfer trend from Ag to graphene can be seen in the Ag/graphene/Ag case due to the lower electron affinity of Ag w.r.t. C. The DP for Ag clusters at the same site is around −0.5eV, which is ~0.1eV higher than the DP around −0.6eV for Ag at different sites. The charge transfer from Ag clusters to graphene is ~0.49e/cell and ~0.75e/cell for the on-site and off-site cases, respectively. The higher DP in the Ag case comparing with the DP of the Cu (Fig. 5(d)) is due to the higher electron affinity of Ag and thus the less charge (electron) transfer from Ag particle to graphene (Fig. 5(f)).

However, it is another story for the Au nanoparticles. Most metals, including Cu and Ag, exhibit lower electron affinity than carbon (C), but in rare cases, Au being one, they have a higher electron affinity. For such cases, the charge transfer is in the

opposite direction, i.e. from graphene to Au clusters as shown in Fig. 5(f and g). This can also be seen in Fig. 5(d and e) that the DPs are higher than E_F, indicating the hole doping nature of the Au case. The DP around 0.09eV for the off-site Au particle case is higher than ~0.03eV for on-site Au clusters (Fig. 5(e)), which means Au clusters can extract more electrons (~0.045e/cell) from graphene if they locate at different sites contacting more C atoms than extracting fewer electrons (~0.030e/cell) from graphene for the on-site Au particle with less Au−C contact (Fig. 5(g)). This is the reason why the calculated total energy is lower for Au clusters at different sites (Fig. 5(c)).

One should notice that the nanoparticles in our experiment are much larger than those in our calculations. To assure our conclusions are correct, at least qualitatively, we can refer to the large-size limit, which corresponds to a monolayer metal film on graphene. A previous work [12] had studied such a system and concluded that the charge transfer is from graphene to Au and from Cu, Ag to graphene, which is exactly the same as those found in our work. This serves as an indirect evidence that our conclusions should be correct for nanoparticles larger in size as well.

In our previous study we have discovered a single nanoparticle of Cu on graphene will also induce surface tension besides charge transfer [11]. However, the main driving force for the above described phenomena are unlikely due to surface tension effect, because the nanoparticle on both sides will draw the same type of force on graphene, either tensile or compressive, which energetically will drive the particles on the two sides to stay away.

4. Conclusions

We have experimentally observed that nanoparticles in the systems of Ag/graphene/Ag and Cu/graphene/Cu display the phenomena of attractive interaction. In the system of Au/graphene/Au, the nanoparticles on the opposite side of graphene prefer to stay away from each other. Our DFT calculations fully support our experimental observations. We further resolve the correlations among the relative total energy, DP energy, and charge transfer for the metal particles moving from the on-site to off-site via first-principles calculations. We clearly demonstrate the close relation between the charge transfer directions with the metal's electron-affinity, and the subsequent attractive/repulsive interactions of the metal clusters through graphene.

Declaration of competing interest

The authors declare that they have no known competing financial interests or personal relationships that could have appeared to influence the work reported in this paper.

Acknowledgements

Appendix A. Supplementary data

Supplementary data to this article can be found online at https://doi.org/10.1016/j.carbon.2020.10.071.

References

[1] S.Z. Butler, S.M. Hollen, L. Cao, Y. Cui, J.A. Gupta, H.R. Gutie rrez, et al., ACS Nano 7 (2013) 2898.
[2] G.R. Bhimanapati, Z. Lin, V. Meunie, Y. Jung, J. Cha, S. Das, et al., ACS Nano 7 (2015) 11509.
[3] W. Yu, M.D. Porosoff, J.G. Chen, Chem. Rev. 112 (2012) 5780.
[4] P. Garcia-Dominguez, C. Nevado, J. Am. Chem. Soc. 138 (2016) 3266.
[5] H.T. Nasrabadi, E. Abbasi, S. Davaran, M. Kouhi, A. Akbarzadeh, Nanomed. Biotechnol. 44 (2016) 376.
[6] K. McNamara, S.A.M. Tofail, Adv. Phys. X 2 (2017) 54.
[7] A. Bansal, S.S. Verma, J. Optic. 45 (2016) 7.
[8] D. Palagin, J.P.K. Doye, Phys. Chem. Chem. Phys. 18 (2016) 22311.
[9] Y. Chen, Q. Zhang, Z. Zhang, X. Zhou, Y. Zhong, M Yang, et al., J. Mater. Chem. 3 (2015) 17874.
[10] M. Sharma, P.R. Pudasaini, F. Ruiz-Zepeda, E. Vinogradova, A.A. Ayon, ACS Appl. Mater. Interfaces 6 (2014) 15472.
[11] L.W. Huang, H.T. Jeng, C.K. Chang, K.H. Chen, F.R. Chen, C.S. Chang, Carbon 98 (2016) 666.
[12] G. Giovannetti, P.A. Khomyakov, G. Brocks, V.M. Karpan, J. van den Brink, P.J. Kelly, PRL 101 (2008), 026803.
[13] K. Xia, H. Zhan, Y. Gu, Procedia IUTAM 21 (2017) 94.
[14] U.N. Maiti, W.J. Lee, J.M. Lee, Y. Oh, J.Y. Kim, J.E. Kim, Adv. Mater. 26 (2014) 40.
[15] Y. Zhu, L. Li, C. Zhang, G. Casillas, Z. Sun, Z. Yan, et al., Nat. Commun. 3 (2012) 1.
[16] C. Tang, Q. Zhang, M.Q. Zhao, G.L. Tian, F. Wei, Nano Energy 7 (2014) 161.
[17] A. Zaleska-Medynska, M. Marchelek, M. Diak, E. Grabowska, Adv. Colloid Interface Sci. 229 (2016) 80.
[18] N. Toshima, T. Yonezawa, New J. Chem. 22 (1998) 1179.
[19] J.Y. Hwang, C.C. Kuo, L.C. Chen, K.H. Chen, Nanotechnology 21 (2010) 465705.
[20] X. Li, Y. Zhu, W. Cai, M. Borysiak, B. Han, D. Chen, et al., Nano Lett. 9 (2009) 4359.
[21] Li-Wei Huang, Cheng-Kai Chang, Fan-Ching Chien, Kuei-Hsien Chen, Peilin Chen, Fu-Rong Chen, Chia-Seng Chang, J. Vac. Sci. Technol., A 32 (2014), 050601.
[22] (Supplementary Information).
[23] P.E. Bl€ochl, Phys. Rev. B 50 (1994) 17953.
[24] G. Kresse, D. Joubert, Phys. Rev. B 59 (1999) 1758.
[25] G. Kresse, J. Hafner, Phys. Rev. B 48 (1993) 13115.
[26] G. Kresse, J. Furthmüller, Phys. Rev. B 54 (1996) 11169.
[27] J.P. Perdew, K. Burke, M. Ernzerhof, Phys. Rev. Lett. 77 (1996) 3865.